ORIGINAL PAPER

CrossMark

Electrochemical noise of a hydrogen-air polymer electrolyte fuel cell operating at different loads

E. A. Astafev[1] · A. E. Ukshe[1] · E. V. Gerasimova[1] · Yu. A. Dobrovolsky[1] · R. A. Manzhos[1] (ID)

Abstract
The electrochemical noise of a polymer membrane hydrogen-air fuel cell operating at different load currents was measured in serial experiments. Spectral power densities of the noise are shown to be divided into three regions. At frequencies greater than 3–10 Hz, the spectrum dependence has a constant slope of -2 in the bilogarithmic coordinates. At frequencies 0.3–5 Hz, there is a horizontal plateau in which length is determined by the value of a load. At frequencies less than 0.3 Hz, the dependence of spectral power density has a slope of -2. Medium-frequency plateau and high-frequency slope of spectral power densities of the noise were approximated by model RC circuits. The values of Faradic resistance and double-layer capacitance connected in parallel were obtained from the electrochemical impedance data. At load voltages higher 0.5 V, the height of the plateau was shown to be proportional to the 2.68 power of the load current value.

Keywords Electrochemical noise · Spectral power density · Equivalent noise resistance · Chemical power sources · Fuel cell

Introduction

The method based on measurement and analysis of electrochemical noise can be placed in one line with other electrochemical methods such as electrochemical impedance and cyclic voltammetry. Today, it is utilized mostly in corrosion measurements [1–6]. However, the method of electrochemical noise is not widely and systematically applied for other electrochemical tasks due to its complexity as in the experimental procedure and requirements to hardware and in the analysis and interpretation of experimental data.

In our opinion [7] and according to other scientists [8], the electrochemical noise method can give the most interesting and essential results if applied for the diagnostics of chemical power sources state of health and estimation of its remaining service life. The first electrochemical noise measurement for chemical power sources has been carried out at the beginning of the second half of the twentieth century [9]. There are several publications on the investigation of fuel cells [7, 10–18] and other batteries [8, 19–22]. It should be mentioned that most authors of these works do not give the answer to the question about the nature of electrochemical noise origin. There are almost no publications except the theoretical ones concerning the precise description of electrochemical noise. In our opinion, most authors do not pay sufficient attention to experimental hardware. Therefore, it is often difficult to interpret its influence on the experiment and obtained data.

Systematical and comprehensive experimental studies of electrochemical noise with the analysis of its nature were held by V.A. Tyagai [23–25]. However, his works, fundamental for the most part, were not concerned the chemical power sources. There are also a lot of publications on the investigation of electrochemical noise by modern scientists [2–4]. In the main, these works are devoted to the corrosion measurements. Recently, a series of works on the theoretical analysis of electrochemical noise caused by thermal fluctuations [26, 27] and the fractal nature of diffusion in the near-electrode layer [28] was published by B.M. Grafov. Besides, he suggested a method of noise analysis with Chebyshev polynomial approximation ("Chebyshev spectrum") [29–31].

The method of electrochemical noise is not so widely used compared to other electrochemical techniques due to a number of technical restrictions. It is the strong requirements to the experimental setup and hardware that hinder the application of the method. For example, low amplitude of electrochemical

✉ E. A. Astafev
tdsipch@list.ru

[1] Institute of Problems of Chemical Physics, RAS, Acad. Semenov av., 1, Chernogolovka, Moscow, Russia 142432

Springer

noise is the reason for the utilization of high-resolution hardware with a low-level self noise [32]; all the components should be thoroughly shielded and grounded.

At the study of a stable electrochemical system when a direct current does not flow, the result of electrochemical noise measurements can be presented as the frequency dependence of real component of the impedance. The method of spectral power density is used in this case, and the power density is converted to the equivalent noise resistance according to the Nyquist equation [33]:

$$R = S_v/4k_bT \qquad (1)$$

where S_v is a spectral power density of the voltage noise, k_b is a Boltzmann constant, T is an absolute temperature, and R is an equivalent noise resistance.

The spectrum of imagine impedance component can be obtained from the frequency dependence of the real impedance component by means of the Kramers-Kronig relation [34]. Thus, the same information as in the electrochemical impedance method can be obtained. The interpretation of results in the case when direct current flows through the electrochemical system is more complex. According to the high number of publications devoted to corrosion studies, there is an amount of experimental data and particular experience of its processing is available. In the case of chemical power sources, the publications do not possess systematical character and the amount of experimental data is low. Moreover, these works only state that electrochemical noise can be applied for diagnostics of chemical power sources.

The goal of the present study is to establish the nature of electrochemical noise for a fuel cell. A hydrogen-air fuel cell is considered as it is virtually the only chemical power source that can operate in near steady-state conditions when the direct current flows in it.

Experimental

The measurements were carried out in the test fuel cell (Electrochem Co.) with working area of 1 cm^2 at 23 °C. The components of membrane electrode assembly were as follows: Nafion® NRE-212 membrane, the catalyst 48.49% Pt/C with Pt load of 0.996 mg/cm^2 (Inenergy Co.), and gas diffusion layer H23C8 (Freudenberg & Co.). Pure hydrogen was utilized as the fuel, air served as the oxidizer. The operation was running in the regime of constant excess flow (15 l per hour) of fuel and oxidizer at 100% humidity. The excess flows were chosen to eliminate their influence on experiment and to minimize the change of oxygen concentration during air pulling through the channels of a fuel cell, as its operation regime is greatly affected by these concentration deviations [16–18]. For example, there could be unpredictable

fluctuations of oxygen concentration near the three-phase interface, which is essentially an extra source of an electrochemical noise. This peculiarity was severely studied in [18].

We have utilized a special-purpose setup for a gas preparation. It included an air pump, a generator of pure hydrogen, a multi-step system of gas humidification and damping of their flows. Besides, all of the elements were shielded and grounded thoroughly. A specialized device NM-4 (Elins, Russia) was utilized as measurement hardware. It was modified additionally for operation with low impedance objects. At frequencies above 50 Hz, it possessed a 1.3-nV/Hz$^{0.5}$ level of self-noise, which is equivalent to the thermal noise of a 100-Ω resistor. The rate of data acquisition was 500 points per second; a data array consisted of 30,000 points. To eliminate the direct current component, the input was equipped with a passive high pass RC-filter (cutoff frequency is of 0.01 Hz) based on high-quality electronic components. Device gain was set to 100 that resulted in a ± 24 mV input range. A setup was tested with high precision constant resistors, for which the registered noise was converted into the thermal noise according to the Nyquist equation.

A scheme of hardware for electrochemical noise measurement is presented in the Fig. 1. The input filter was made of 16 ceramic capacitors Murata GRM32ER60J107ME20L, 100 μF, 6.3 V assembled in parallel by means of suspended mount to prevent piezoelectric effect. The filter resistor R_F was Yageo thin film 0.1% 15 ppm precision resistor 1/6 W, 10 K MFP-12BTC52. The resistors of the same type were utilized as a load; resistors of 1 kΩ were connected in parallel to obtain 333 Ω load. C2-23 2 W 5% 100 Ω metal oxide resistors were used as 100 Ω load and three ones in parallel as 33 Ω load. Ten Ω load and the ones of a lower resistance were combined from SQP-5 5 W 5% wire resistors in such way that power dissipated on every resistor did not exceed 1/20 of its nominal power. When load resistor was connected to a fuel cell, the drop of a load voltage was observed. Therefore, not to saturate high gain amplifier A1, R_F resistor was shorted for a few seconds by 1 Ω resistor to let the C_F capacitor charge (the filter was set fast to the voltages that would not saturate amplifier A1). Then, 1 Ω shorting resistor was removed and a fuel cell reached steady-state condition.

At the stage of processing of measured data, the spectral power density of the measurement device self-noise was subtracted from the spectral power density of the object noise. The hardware self-noise was measured on every device turn-on and warming-up.

The electrochemical noise measurements were conducted in series at a variation of the load (see Table 1). Prior to noise measurement for every load, a fuel cell was operated during 1 h to approach a near steady-state condition. After electrochemical noise measurement step, a voltage drop on load resistor was measured by V7-78/1 digital voltmeter (Protech Co.). Then, the load current was calculated according to the
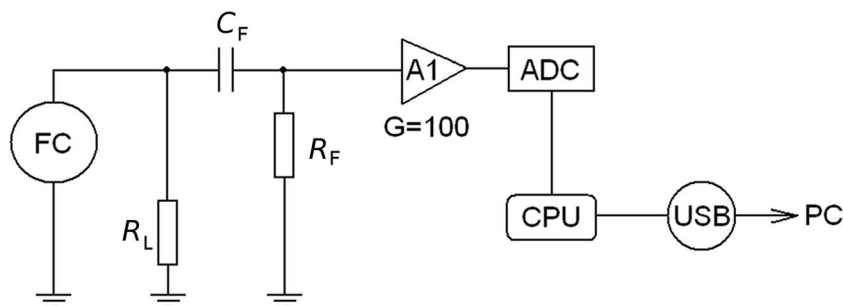
Fig. 1 A scheme of hardware for electrochemical noise measurement. FC—fuel cell under test, R_L—load resistor, C_F—filter capacitor, R_F—filter resistor, A1—ECN amplifier with gain 100, ADC—analog to digital converter, CPU—ARM3-based microcontroller for IO operations and control, USB—galvanically isolated USB interface and power unit

Ohm law. Thereafter, an electrochemical impedance was measured at load voltage achieved for every load resistor.

Figure 2 shows typical electrochemical noise measured for several loads. The data denotes initial signal without application of any detrending procedure, i.e. without subtraction of a slowly drifting "constant" component of the measured voltage. The absolute values are shifted to some extent to improve the representation of curves. As it can be seen, the amplitude of electrochemical noise becomes greater with the increase in the load. Besides, a self-noise of the device is also presented in the figure. Visually self-noise is more linear, the trend is weak, and the amplitude is smaller.

A P-40X potentiostat (Elins Co.) with the FRA-24M frequency response analyzer module was applied in electrochemical impedance measurements. They were carried out in a potentiostatic regime. The amplitude of AC signal was 5 mV. Prior to electrochemical impedance measurement, a fuel cell was polarized at load voltage during 1 h to approach a near steady-state condition. The Nyquist plots of impedance are presented in the Fig. 3.

As can be seen from the Fig. 3 and its inset, the impedance spectra for plots 6 and 7 contains a high-frequency arc corresponding to charge transfer resistance and double-layer capacitance. At low frequencies, it transforms into a circle with linear initial section which corresponds to the diffusion mass transport in porous electrode. Fitting confirms this interpretation [35]. The curve 8 in the Fig. 3 demonstrates an increase in total impedance and in charge transfer resistance, in particular,

at high load current. This phenomenon was observed earlier in our work [36] and in [17, 37].

Data processing and analysis of results

From the obtained data arrays of electrochemical noise, frequency dependencies of spectral power densities were calculated. The latter were transformed into equivalent noise resistance according to the Nyquist Eq. (1) to improve the representation of the data and compare it with the real component of the impedance obtained by the impedance spectroscopy method.

Before spectral power density calculation, an array of noise data consisting of 250,000 points was divided into 10 segments of 25,000 points. Linear trend removal procedure using first-order polynomial fitting was applied to every segment independently. Then, a spectral power density was calculated for every segment and then ten resulting spectral power densities were averaged to obtain final power spectrum presented in the Fig. 4. Discrete Fourier transform was used for spectral power density calculation. Lowest frequency point of every

Table 1 The values of a fuel cell operation voltage and current for every load resistor

R (Ω)	E (V)	I (A)
333	0.824	0.0025
100	0.794	0.0079
33	0.748	0.0227
10	0.69	0.069
3.2	0.62	0.194
1	0.5	0.5
0.27	0.287	1.063
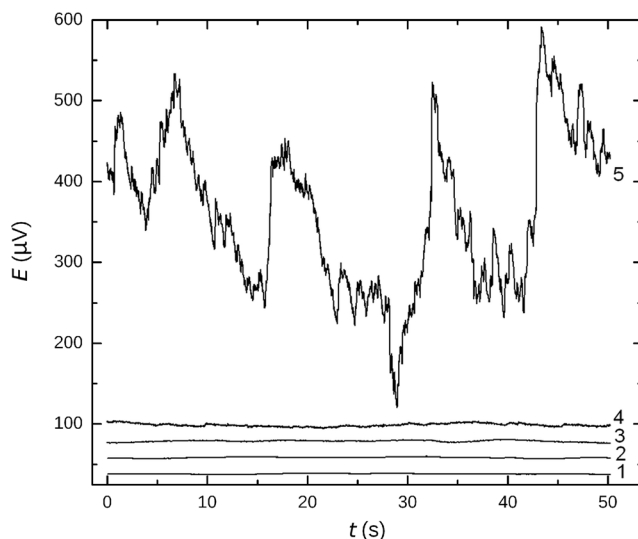
Fig. 2 Electrochemical noise measured at different constant fuel cell loads, Ω: 2—333, 3—33, 4—3.3, 5—0.27. 1—noise of the device

Fig. 3 The Nyquist plots of an impedance at different load voltages, V: 1—0.98 (open circuit potential), 2—0.824, 3—0.794, 4—0.748, 5—0.69, 6—0.62, 7—0.5, 8—0.287. Inset shows Nyquist plots 6 and 7 in more details
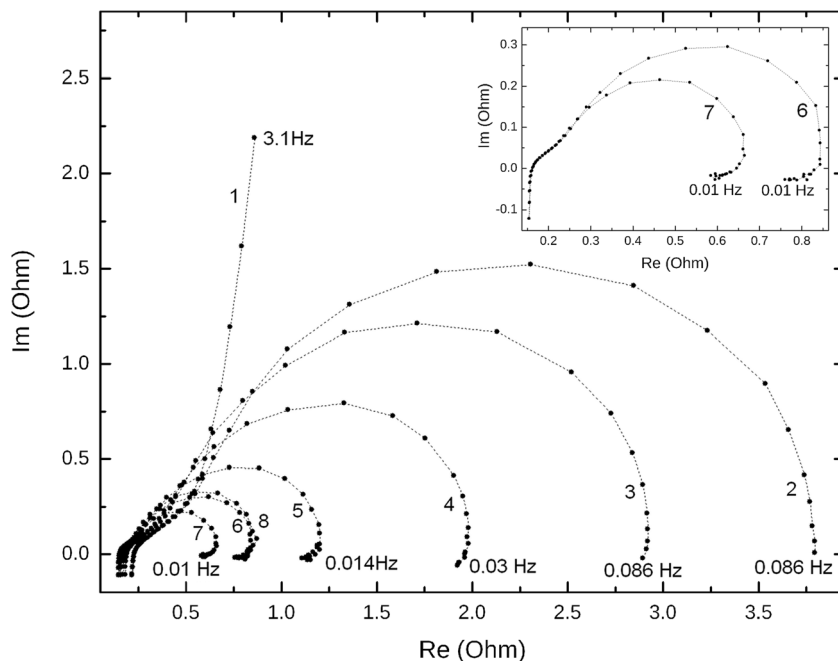
curve was removed since it was affected by detrending procedure and input analog filter. All computation algorithms were carefully tested and approved by measurements of precision resistor thermal noise in the course of hardware and software validation [38, 39].

Frequency dependencies of equivalent noise resistance at different load currents are presented in the Fig. 4 in logarithmic coordinates. The spectra of the real component of impedance and a self-noise of the device are presented for comparison.

As it can be seen from the figure, at frequencies higher than 1–10 Hz (depending on the operation voltage), the obtained frequency dependencies are straight lines with a slope close to 2. For example, at the maximum load voltage of 0.287 V, the slope equals to 2 at frequencies more than 1 Hz. With the increase in load current, there is a near parallel shift of frequency dependencies into the region of higher values of equivalent noise resistance.

In the region of medium frequencies from 0.3 to 5 Hz, the majority of curves are deviating from the linear ones (in

Fig. 4 The spectra of equivalent noise resistance of a fuel cell at different load voltages (upper curves) and the corresponding real components of electrochemical impedance (lower curves of the same color), V: 1—0.794, 2—0.748, 3—0.69, 4—0.62, 5—0.5, 6—0.287. 7—a self-noise of the device with the short-circuited input filter. The curves (1–6) of equivalent noise resistance were obtained after subtraction of the device noise (7)
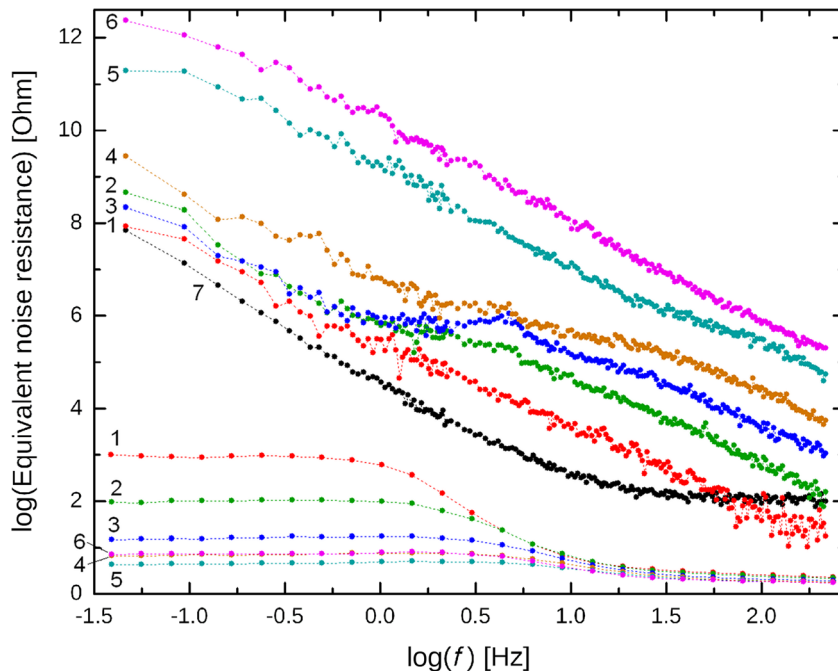
logarithmic coordinates) with the decrease in slope and approaching a small plateau. Meanwhile, with the increase in the load, this deviation shifts to the lower frequencies. The most pronounced plateau is observed for curve 3 at medium load. The less pronounced plateau is the feature of curves 2 and 4. For curve 5, it is even less, and dependencies 1 and 6 have a slightly visible distortion. The same behavior is typical for corrosion systems. In these systems, a slope of − 2 is observed at high frequencies, and a horizontal plateau represents itself at low frequencies, but the second low-frequency slope at low frequencies is not observed [3, 5, 40].

At frequencies less than 0.1 Hz, there is a deviation from the linear low-frequency slope of 2. This deviation is caused by the influence of the device input filter with cutoff frequency of 0.01 Hz. For the maximum load of a fuel cell (curve 3 in the Fig. 3), the slope of spectral power density is 2.11 in the frequency region of 0.15 to 0.86 Hz. The same slope is observed for a 100 Ω load (curve 1 in the Fig. 3) in the frequency region of 0.1 to 1.1 Hz.

Detailed information about slopes of equivalent noise resistance spectra is presented in the Table 2. The mid-frequency plateau and low-frequency slope were difficult to determine with good accuracy at 0.824 V load. That is why data for this load are not shown in the table. Besides, the mid-frequency plateau was difficult to isolate at the strongest 0.287 V load. For this load, only high- and low-frequency slopes are represented. At high frequencies, the curves corresponding to 0.824 and 0.794 V are bounded by the plateau of device noise. Consequently, these high-frequency bounds are lower than the ones for other curves, namely these bounds are 27 and 102 Hz, respectively.

A linear dependence of spectral power density on frequency was observed in [14], but its slope was close to 1.3 at medium frequencies and increased up to 2.9 at frequencies higher than 0.5 Hz. In [12], there was also a linear frequency dependence of spectral power density of voltage noise with the slope of 2.5–3. Besides, at the frequency of 2 Hz, there was a linear plateau at any fuel cell load. The difference in the slope from our observations is probably connected with the peculiarities of the hardware used by the authors of the work [14]; moreover, the fuel and oxidizer were taken in stoichiometric quantities, not the excess ones as in the present study. Moreover, the difference may be caused by the usage of pure oxygen, not air. It should be mentioned that in one of the latest works on the discussed subject [13], the slope of spectral power density of voltage noise of an operating fuel cell also equals to 2. In the works [13, 15] performed by two groups in collaboration, there was also a deviation from the linear dependencies of noise spectral power density. In our previous work [7], the slopes of the spectral power density of a fuel cell were close to 2 down to frequencies about 1 mHz, which was attained by the utilization of hardware with direct high-sensitivity measurement circuit without any input filters [32].

It should be noted that frequency dependencies of the real impedance component not only possess a different slope and shape but also have several orders of magnitude lower level at all load voltages. First of all, it argues for a considerable excess noise in the system. Second, the nature of this noise differs significantly from the thermal one. Besides, it is not related to a traditional shot noise, because the latter does not reveal such frequency dependence [41]. On the other hand, in many systems, there is such phenomenon as flicker-noise. Ordinary flicker-noise has the characteristic slope of − 1, which corresponds to the diffusion nature of dissipation of random inhomogeneities. However, large slopes up to − 2 are possible in the case of Levi's diffusion [42].

Electrochemical noise is most often identified as a thermal noise of Faradic resistance of electrochemical reaction. It is usually shunted by an electric double-layer capacitance with a model noise source [5, 6]. Appropriate circuits with a generator of noise current—b and noise voltage—c are presented in the Fig. 5. This model corresponds to a thermal noise incorporated into an equivalent circuit of a double layer according to an equivalent generator theorem [43]. In that case, the frequency characteristic of the electrochemical system is described by the parallel RC circuit:

$$i_n^2 = U_0^2 \cdot \left(\frac{1}{R_F^2} + (\omega C)^2 \right) \tag{2}$$

Table 2 The values of slopes of equivalent noise resistance spectra and corresponding frequency ranges for different loads of a fuel cell

E (V)	High-frequency slope	High-frequency range (Hz)	Mid-frequency slope	Mid-frequency range (Hz)	Low-frequency slope	Low-frequency range (Hz)
0.824	− 1.92	27–0.05	–	–	–	–
0.794	− 1.88	102–2.20	− 1.51	2.20–0.5	− 2.20	0.5–0.05
0.748	− 1.87	209–4.57	− 0.78	4.57–0.9	− 2.35	0.9–0.05
0.69	− 1.64	209–5.22	− 0.032	5.22–0.9	− 2.00	0.9–0.05
0.62	− 1.63	209–16.2	− 0.99	16.2–2.09	− 1.86	2.09–0.05
0.5	− 1.54	209–19.9	− 2.12	19.9–6.31	− 2.18	6.31–0.15
0.287	− 2.06	209–12.1	–	–	− 2.12	12.1–0.15
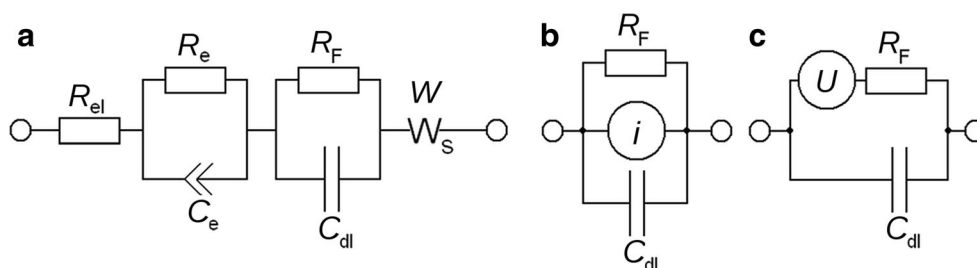
Fig. 5 **a** An equivalent circuit of a fuel cell. R_{el} is a resistance of the electrolyte; R_e is a resistance of distributed interface with corresponding distributed capacitance C_e. R_F is a Faradic resistance, C_{dl} is a double-layer capacitance for the cathode, and W is a diffusion impedance of oxygen transport to the three-phase interface. **b**, **c** Equivalent circuits with current and voltage noise sources

In logarithmic coordinates, a frequency dependence of noise power for such a model looks like the following:

$$\log(i_n^2) = 2 \cdot \log(U_0) + \log\left(\frac{1}{R_F^2} + (\omega C)^2\right) \quad (3)$$

Equation (2) is divided into two ranges of frequencies. If $\omega C >> 1/R_F$, then:

$$\log(i_n^2) = 2 \cdot \log(U_0) + 2 \cdot \log(\omega C) \quad (4)$$

If $\omega C << 1/R_F$, then:

$$i_n = \frac{U_0}{R_F}, \log(i_n^2) = 2 \cdot \log(U_0) - 2 \cdot \log(R_F) \quad (5)$$

Thus, at low frequency, the spectrum is independent of frequency (approaches a plateau).

To test this model with obtained frequency dependencies of spectral power density, the values of Faradic resistance and double-layer capacitance were calculated from the electrochemical impedance data. The results are presented in Table 3. The calculation was performed by means of the analysis of equivalent circuits. An equivalent circuit a is presented in the Fig. 5. In the last column of Table 3, the time constants of RC circuits obtained from the calculated values of double-layer capacitance and Faradic resistance are presented. Below the frequencies corresponding to them, there is a deviation of frequency characteristic from the linear slope of -2 with the approaching to the horizontal

Table 3 The values of Faradic resistance, double-layer capacitance, and cutoff frequency of parallel RC circuit calculated from the equivalent circuit analysis

E (V)	R_F (Ω)	C_{dl} (F)	f (Hz)	τ (s)
0.824	8.53	0.05	0.37	2.7
0.794	2.025	0.052	1.51	0.662
0.748	0.687	0.055	4.21	0.237
0.69	0.309	0.078	6.60	0.151
0.62	0.157	0.08	12.7	0.079
0.5	0.1479	0.061	17.6	0.0567
0.287	0.338	0.059	7.98	0.125

frequency dependence (5). Above the corresponding frequencies, the slope of spectral power density of this RC circuit frequency characteristic equals to -2 (4) as at high frequencies for the examined system.

For every load voltage, the calculated values of double-layer capacitance and Faradic resistance were used for approximation of noise spectral power densities. The calculated curves approximating equivalent noise resistances are presented in the Fig. 6. The values of capacitance and resistance were selected to satisfy the time constant of RC circuit consisted of double-layer capacitance and Faradic resistance for every load voltage. The bottom curve in the Fig. 5, which corresponds to the lowest load at 0.824 V, approaches a horizontal plateau in the region of frequencies higher than 40 Hz. It is caused by the hardware limitations, i.e. by the self-noise of the device. In fact, after subtraction of the self-noise, spectral power density is still limited by the hardware and does not approach its logical end, i.e. a thermal noise of the real component of the equivalent circuit. To a lesser degree, the same phenomenon is observed at high frequencies for spectral power density at a load of 0.794 V.

As it can be seen from the Table 3, the frequencies at which the deviation from the linear slope of -2 and the approach to the horizontal line must take place are in the examined frequency region. However, there is no transition to the horizontal low-frequency slope at frequencies below 0.3–3 Hz (depending on the curve number). This feature argues that the slope of -2 at frequencies lower than 0.3–3 Hz is caused by other factors than at frequencies higher than 10 Hz.

It should be mentioned that the problem of correct mathematical model selection for a precise description of electrochemical noise is connected with the limits of working frequencies. The wider frequency region is used for noise measurement, the more comprehensive description of the system is available. This feature makes the method of electrochemical noise similar to the electrochemical impedance for which the frequency region is the primary factor that determines the results of the measurement [36, 44].

To summarize the discussion of frequency dependencies of the equivalent noise resistance, let us consider the operation of a fuel cell at 0.69 V. The appropriate spectrum is presented in

Fig. 6 Approximation (solid black lines) of spectral power densities by the parallel RC circuits with time constants determined from the impedance data (Table 2) at different load voltages, V: 1—0.824, 2—0.794, 3—0.748, 4—0.62, 5—0.5, 6—0.287
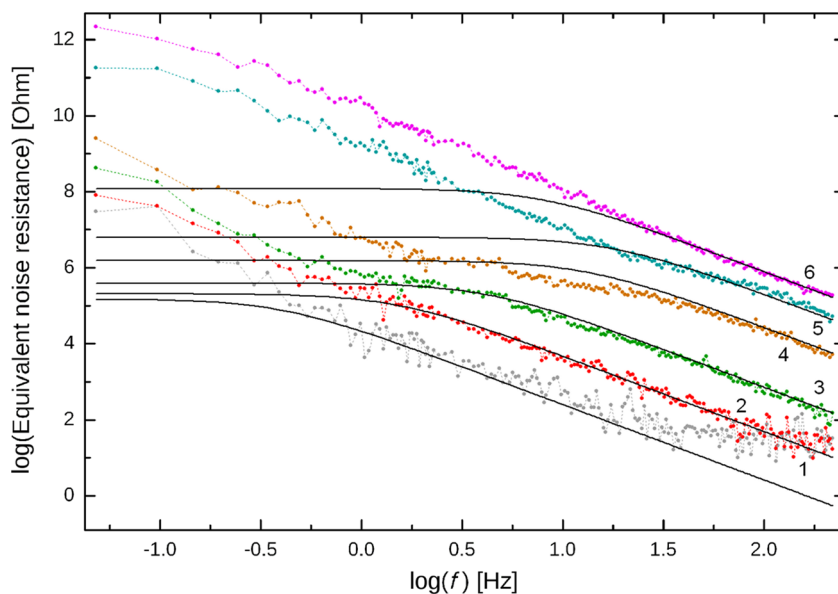
the Fig. 7. The approximation by RC circuit has been performed at frequencies higher than 0.9 Hz, and additional linear approximation has been performed in the region of low frequencies from 0.1 to 0.9 Hz. The low-frequency straight line has the slope of 2.03. In addition to two slopes discussed above and a plateau between them, there is a maximum on the curve at 4.8 Hz. Similar effects were studied by modeling and analysis of frequency dependencies of single and distributed in time splashes in corrosion systems [45, 46]. The presence of these resonances evidence that in noisy system there is no random time distribution but splashes with some characteristic time which generates the noise. We have already observed analogous resonances at sufficiently low frequencies during the study of the noise of a fuel cell operating without a

load [7]. These resonances were reproduced in two sequential experiments carried after fuel cell relaxation for 12 h. The hardware was validated too by recording its noise with shorted input. These experiments were repeated to verify the nature of spectral power densities.

A little drop of spectral power density at frequencies higher than the frequency of the maximum is also predicted by calculations in [45]. To a lesser degree, a similar phenomenon is observed for curve 4 (brown) in the Fig. 6. Characteristic transients which probably determine the nature of noise spectral power density can be observed for the lowest load on the noise signal itself in the Fig. 2. A typical shape (abrupt front and exponential decay) of these transients was modeled mathematically in [45].

Fig. 7 Spectral power density of noise at load voltage of 0.69 V—1. Its approximation in the region of medium and high frequencies (AB)—2 and in the region of low frequencies (C)—3. The slope of the curve in 0.1–0.9 Hz region is −2.03
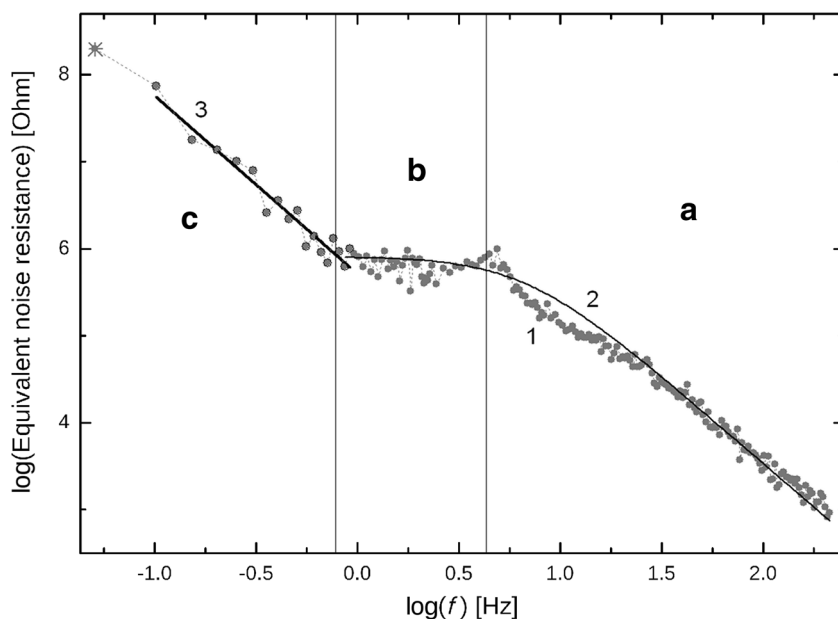
To investigate the "amplitude" dependence of the registered noise, frequency dependencies of spectral power densities of an electrochemical noise of current were calculated, and their dependency on the load current was plotted. In bilogarithmic coordinates, the dependency appeared to be quite linear in the region of the high-frequency linear slope of − 2 (region C). Thus, for example, the result of linear approximation at 210 Hz in the "logarithm of spectral power density of the current–logarithm of direct current" coordinates is a slope of 4.0133 with standard deviation of 0.9893 (Fig. 8). This tendency was observed for every processed frequency up to 10 Hz, but at low frequencies, there were a little deviation at maximum load currents. As it were in the case of frequency dependencies, the amplitude dependencies calculated for different frequencies are parallel to each other (Fig. 8). A little deviation from linear dependence at low currents is due to the self-noise of the device. The value of the slope of amplitude dependence indicates that the values of the spectral power density of electrochemical noise of current are proportional to the fourth power of the load direct current of a fuel cell for the same frequency in the considered frequency region.

The dependence of equivalent resistor values used for noise spectral power density approximation (Fig. 6) with RC circuits on the values of load current is presented in the Fig. 9. Contrary to the Fig. 8, in which noise corresponds to high frequencies greater than 10 Hz, the data in the Fig. 9 describes the height of medium-frequency plateau in the 0.3–5 Hz frequency region. As it is seen, there is a linear part at low loads; it consists of five points and can be approximated by the line with a slope of 2.68. In our opinion, the analysis of amplitude dependencies at lower frequencies is not worthwhile. The difference in amplitude dependencies at low (< 0.3 Hz) and high

(> 10 Hz) frequencies, as well as the results of the analysis of frequency dependencies (Fig. 6), is a sign of different noise natures at these frequencies.

The noise at low frequencies can be explained by the specific features of formation of a new phase and removal of the reaction product. Some ideas that problems and features of water management can affect electrochemical noise were mentioned in [15]. We assume that fluctuations can be the result of removal of the reaction product, i.e., water. Water droplets can locally shield a three-phase boundary. This shielding is limited in time by the processes of formation and growth of water droplets. The nature of noise in this situation can probably be explained in the same way as generation-recombination noise [47], which demonstrates − 2 slope of the frequency dependence in the frequency range, which in our case might depend on the growth time of the water droplets. It seems to us that the period of water droplet growth can be assumed to be equivalent to the charge lifetime period in the theory of generation-recombination noise. During the period of water droplet growth, a certain region of three-phase boundary at the cathode is shielded. This means that a certain charge is not transferred through this boundary during the period of water droplet growth as compared with a situation when the boundary is not shielded. This virtual charge is equivalent to the charge value, which is used in the theory of generation-recombination of noise. Modeling of electrochemical noise of formation of new phases was investigated using similar ideas in [48]. Modeling these situations is one of the interests of our future work.

The establishment of the relation of impedance data with the electrochemical noise is of a great interest. At frequencies greater than 200 Hz, the main contribution in impedance is

Fig. 8 Spectral power densities of current noise depended on the load current for two high frequencies: 34 and 210 Hz ("amplitude dependence")
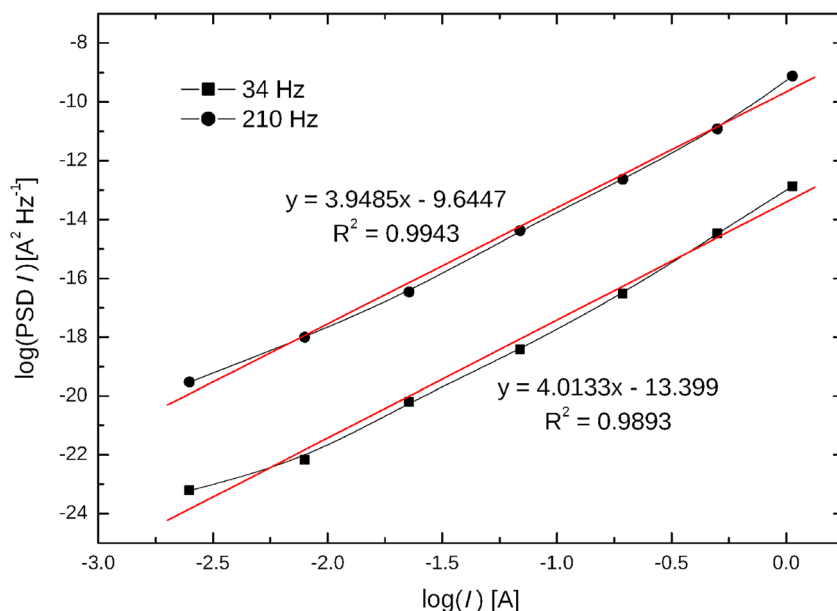
Fig. 9 The logarithm of the low-frequency plateau height on RC circuit approximations of the spectral power density of current noise depended on the logarithm of direct current. The approximation of five bottom points gives a slope of 2.68 at 0.9986 reliability
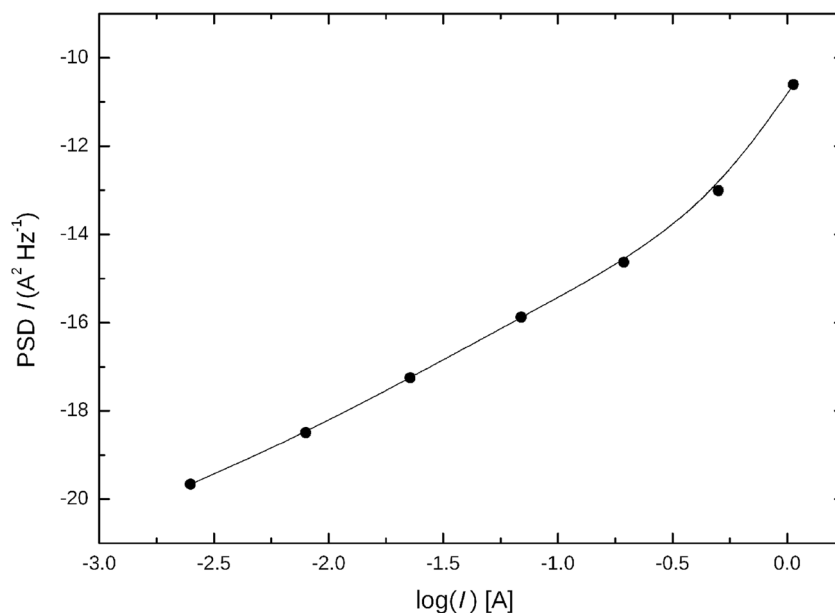
done by the distributed properties of high porosity electrode–electrolyte interface based on the carbon support [44, 49–51]. This frequency region is unavailable in our noise experiment.

At low frequencies, the nature of impedance and spectral power density spectra is determined by common elements of the equivalent circuit, which are double-layer capacitance and Faradic resistance. At frequencies less than 0.3 Hz before the influence of sub low-frequency inductance-like feature [17, 50], the nature of impedance spectrum is determined by diffusion phenomenon, which is the case for an explanation of the nature of noise. However, there are principal differences. As frequency approaches zero, the impedance approaches a finite value on the real axis. At the same time, spectral power density continues to grow even at the minimal frequency in the experiment. This phenomenon is observed in the majority of works on this thematic [7, 13–15]. And there is still no exact explanation of this phenomenon, but only an assumption about diffusion.

A medium-frequency plateau in the 0.3 to 10 Hz region that is a typical separator between high-frequency kinetic RC circuit of double-layer capacitance and Faradic resistance and a low-frequency diffusion contribution observed preferentially in 0.7 to 0.5 V voltage region. That is in the region of mixed kinetics, where an electrochemical reaction of oxygen redaction at the cathode of a fuel cell is limited both by the electron transfer stage and by oxygen diffusion. At the Nyquist plots of impedance, the transition from the half circle formed by double-layer capacitance and Faradic resistance to the low-frequency diffusion features is known to occur with smaller or bigger separation for different loads [16, 17, 36, 37, 44, 49–52]. It can be observed visually on the Nyquist plots of

an impedance or mathematically as the results of equivalent circuit approximations.

Conclusions

The electrochemical noise of a polymer membrane hydrogen-air fuel cell operating at different load currents was measured in serial experiments.

Spectral power densities of the noise were calculated for different loads. Their frequency dependencies are shown to be divided into three regions. At frequencies greater than 3–10 Hz, there is a constant slope of -2. At frequencies 0.3–5 Hz, there is a horizontal plateau which length is determined by the value of a load. The most probable reason for this phenomenon is a shunting of the source of electrochemical noise that is a Faradic resistance with a double-layer capacitance. At frequencies less than 0.3 Hz, the dependence of spectral power density has a slope of -2 again. The most probable explanation of this slope is a diffusion of oxygen and water.

The dependencies of the spectral power density of electrochemical noise of current of a fuel cell on the value of load current were obtained for frequencies up to 10 Hz. They appeared to be proportional to the fourth power of load current of a fuel cell.

From the electrochemical impedance data, the values of time constants were obtained for Faradic resistance and double-layer capacitance connected in parallel. These values were used for the approximation of medium-frequency plateau and high-frequency slope of spectral power densities of the noise by model RC circuits. At load voltages higher than 0.5 V, the height of the plateau was shown to be proportional to the 2.68 power of the load current value.

References

1. Liu L, Li Y, Wang F (2008) Pitting mechanism on an austenite stainless steel nanocrystalline coating investigated by electrochemical noise and *in-situ* AFM analysis. Electrochim Acta 54(2):768–780. https://doi.org/10.1016/j.electacta.2008.06.076

2. Bertocci U, Huet F, Nogueira RP, Rousseau P (2002) Drift removal procedures in the analysis of electrochemical noise. Corrosion 58(4):337–347. https://doi.org/10.5006/1.3287684

3. Oltra R, Gabrielli C, Huet F, Keddam M (1986) Electrochemical investigation of locally depassivated iron. A comparison of various techniques. Electrochim Acta 31(12):1505–1511. https://doi.org/10.1016/0013-4686(86)87068-2

4. Ritter S, Huet F, Cottis RA (2012) Guideline for an assessment of electrochemical noise measurement devices. Mat Corros 63(4):297–302. https://doi.org/10.1002/maco.201005839

5. Singh PS, Lemay SG (2016) Stochastic processes in electrochemistry. Anal Chem 88(10):5017–5027. https://doi.org/10.1021/acs.analchem.6b00683

6. Bertocci U, Huet F (1995) Noise analysis applied to electrochemical systems. Corrosion 51(2):131–144. https://doi.org/10.5006/1.3293585

7. Astafev EA, Ukshe AE, Manzhos RA, Dobrovolsky YA, Lakeev SG, Timashev SF (2017) Flicker noise spectroscopy in the analysis of electrochemical noise of hydrogen-air PEM fuel cell during its degradation. Int J Electrochem Sci 12:1742–1754

8. Martemianov S, Adiutantov V, Evdokimov YK, Madier L, Maillard F, Thomas A (2015) New methodology of electrochemical noise analysis and applications for commercial Li-ion batteries. J Solid State Electrochem 19(9):2803–2810. https://doi.org/10.1007/s10008-015-2855-2

9. Knott KF (1965) Measurement of battery noise and resistor-current noise at subaudio frequencies. Electron Lett 1(5):132. https://doi.org/10.1049/el:19650123

10. Rubio MA, Bethune K, Urquia A, St-Pierre J (2016) Proton exchange membrane fuel cell failure mode early diagnosis with wavelet analysis of electrochemical noise. Int J Hydrog Energy 41(33):14991–15001. https://doi.org/10.1016/j.ijhydene.2016.05.292

11. Koshekov KT, Klikushin YN, Kobenko VY, Evdokimov YK, Demyanenko AV (2014) Fuel cell diagnostics using identification measurement theory. J Fuel Cell Sci Technol 11:051003-1–051003-9

12. Legros B, Thivel PX, Bultel Y, Nogueira RP (2011) First results on PEMFC diagnosis by electrochemical noise. Electrochem Commun 13(12):1514–1516. https://doi.org/10.1016/j.elecom.2011.10.007

13. Maizia R, Dib A, Thomas A, Martemianov S (2017) Proton exchange membrane fuel cell diagnosis by spectral characterization of the electrochemical noise. J Power Sources 342:553–561. https://doi.org/10.1016/j.jpowsour.2016.12.053

14. Evdokimov YK, Denisov ES, Martemianov SA (2009) Electrical noise of hydrogen fuel cell and diagnostic characteristic research. Nonlinear World 7:706–713

15. Denisov ES, Evdokimov YK, Martemianov S, Thomas A, Adiutantov N (2017) Electrochemical noise as a diagnostic tool for PEMFC. Fuel Cells 17(2):225–237. https://doi.org/10.1002/fuce.201600077

16. Cruz-Manzo S, Chen R, Rama P (2013) Study of current distribution and oxygen diffusion in the fuel cell cathode catalyst layer through electrochemical impedance spectroscopy. Int J Hydrog Energy 38(3):1702–1713. https://doi.org/10.1016/j.ijhydene.2012.08.141

17. Bao C, Bessler WG (2015) Two-dimensional modeling of a polymer electrolyte membrane fuel cell with long flow channel. Part II. Physics-based electrochemical impedance analysis. J Power Sources 278:675–682. https://doi.org/10.1016/j.jpowsour.2014.12.045

18. Niroumand AM, Mérida W, Eikerling M, Saif M (2010) Pressure–voltage oscillations as a diagnostic tool for PEFC cathodes. Electrochem Commun 12(1):122–124. https://doi.org/10.1016/j.elecom.2009.11.003

19. Baert DHJ, Vervaet AAK (2003) Small bandwidth measurement of the noise voltage of batteries. J Power Sources 114(2):357–365. https://doi.org/10.1016/S0378-7753(02)00599-2

20. Martinet S, Durand R, Ozil P, Leblanc P, Blanchard P (1999) Application of electrochemical noise analysis to the study of batteries: state-of-charge determination and overcharge detection. J Power Sources 83(1-2):93–99. https://doi.org/10.1016/S0378-7753(99)00272-4

21. Roberge P, Beaudoin R (1989) Voltage noise measurements on sealed lead-acid batteries. J Power Sources 27(2):177–186. https://doi.org/10.1016/0378-7753(89)80131-4

22. Martemianov S, Maillard F, Thomas A, Lagonotte P, Madier L (2016) Noise diagnosis of commercial Li-ion batteries using high-order moments. Russ J Electrochem 52(12):1122–1130. https://doi.org/10.1134/S1023193516120089

23. Tyagai VA, Luk'yanchikova NB (1967) Equilibrium fluctuations in electrochemical processes. Elektrokhimiya 3:316–322

24. Tyagai VA (1971) Faradaic noise of complex electrochemical reactions. Electrochim Acta 16(10):1647–1654. https://doi.org/10.1016/0013-4686(71)85075-2

25. Tyagai VA (1974) Noise in electrochemical systems. Elektrokhimiya 10:3–24

26. Grafov BM (1966) On the equilibrium fluctuations in a stationary state. Elektrokhimiya 2:1249–1253

27. Grafov BM (2011) Gibbs fluctuation theory in the context of electrochemical equilibrium noise. Pure Appl Chem 83:253–257

28. Grafov BM (2015) Fractal theory of electrochemical diffusion noise. Russ J Electrochem 51(1):1–6. https://doi.org/10.1134/S1023193515010073

29. Grafov BM, Dobrovol'skii YA, Davydov AD, Ukshe AE, Klyuev AL, Astaf'ev EA (2015) Electrochemical noise diagnostics: analysis of algorithm of orthogonal expansions. Russ J Electrochem 51(6):503–507. https://doi.org/10.1134/S1023193515060063

30. Klyuev AL, Davydov AD, Grafov BM, Dobrovolskii YA, Ukshe AE, Astaf'ev EA (2016) Electrochemical noise spectroscopy: method of secondary Chebyshev spectrum. Russ J Electrochem 52(10):1001–1005. https://doi.org/10.1134/S1023193516100062

31. Grafov BM, Dobrovolskii YA, Klyuev AL, Ukshe AE, Davydov AD, Astaf'ev EA (2017) Median Chebyshev spectroscopy of electrochemical noise. J Solid State Electrochem 21(3):915–918. https://doi.org/10.1007/s10008-016-3395-0

32. Astaf'ev EA, Ukshe AE, Dobrovolskii YA (2017) Hardware for measurement of electrochemical noise of chemical power sources. Instrum Exp Tech 60:130–131. https://doi.org/10.7868/S0032816217050032

33. Nyquist H (1928) Thermal agitation of electric charge in conductors. Phys Rev 32(1):110–113. https://doi.org/10.1103/PhysRev.32.110

34. Kramers HA (1927) La diffusion de la lumiere par les atoms. Atti Congr Inten Fis Como 2:545–557

35. Yuan X, Wang H, Sun JC, Zhang J (2007) AC impedance technique in PEM fuel cell diagnosis—a review. Int J Hydrog Energy 32(17):4365–4380. https://doi.org/10.1016/j.ijhydene.2007.05.036

36. Astaf'ev EA, Lyskov NV, Gerasimova EV (2009) Research of polymer electrolyte fuel cell cathodes by electrochemical techniques. Int Sci J Altern Energy Ecol 8:93–101

37. Antonacci P, Chevalier S, Lee J, Ge N, Hinebaugh J, Yip R, Tabuchi Y, Kotaka T, Bazylak A (2016) Balancing mass transport resistance and membrane resistance when tailoring microporous layer thickness for polymer electrolyte membrane fuel cells operating at high

current densities. Electrochim Acta 188:888–897. https://doi.org/10.1016/j.electacta.2015.11.115

38. Astaf'ev EA (2018) Multi-purpose high resolution device for measurement of electrochemical noise. Instrum Exp Tech 61. https://doi.org/10.7868/S0032816218010123

39. Astaf'ev EA, Manzhos RA (2018) Wide dynamic range hardware for electrochemical noise measurement. Instrum Exp Tech 61:149–150. https://doi.org/10.7868/S0032816217060192

40. Homborg AM, Tinga T, van Westing EPM, Zhang X, Ferrari GM, de Wit JHW, Mol JMC (2014) A critical appraisal of the interpretation of electrochemical noise for corrosion studies. Corrosion 70(10):971–987. https://doi.org/10.5006/1277

41. Schottky W (1918) Über spontane Stromschwankungen in verschiedenen Elektrizitätsleitern. Ann Phys 57:541–567

42. Timashev SF, Polyakov YS (2007) Review of flicker noise spectroscopy in electrochemistry. Fluct Noise Lett 7(02):R15–R17. https://doi.org/10.1142/S0219477507003829

43. Beletskiy AF (1967) An introduction to the principles of linear circuits. Svyaz, Moscow

44. Barsoukov E, Macdonald JR (eds) (2005) Impedance spectroscopy: theory, experiment, and applications, 2nd edn. Hoboken, Wiley. https://doi.org/10.1002/0471716243

45. Bertocci U, Huet F, Jaoul B, Rousseau P (2000) Frequency analysis of transients in electrochemical noise: mathematical relationships and computer simulations. Corrosion 56(7):675–683. https://doi.org/10.5006/1.3280570

46. Cheng YF, Luo JL, Wilmott M (2000) Spectral analysis of electrochemical noise with different transient shapes. Electrochim Acta 45(11):1763–1771. https://doi.org/10.1016/S0013-4686(99)00406-5

47. Burgess RE (1956) The statistics of charge carrier fluctuations in semiconductors. Proc Phys Soc B 69(10):1020–1027. https://doi.org/10.1088/0370-1301/69/10/308

48. Gabrielli C, Huet F, Nogueira RP (2005) Fluctuations of concentration overpotential generated at gas-evolving electrodes. Electrochim Acta 50(18):3726–3736. https://doi.org/10.1016/j.electacta.2005.01.019

49. Shinozaki K, Zack JW, Pylypenko S, Pivovar BS, Kocha SS (2015) Oxygen reduction reaction measurements on platinum electrocatalysts utilizing rotating disk electrode technique. II. Influence of ink formulation, catalyst layer uniformity and thickness. J Electrochem Soc 162(12):F1384–F1396. https://doi.org/10.1149/2.0551512jes

50. Astafiev EA, Dobrovol'sky YA, Gerasimova EV, Arsatov AV (2008) Special methodological aspects of studying fuel cell electrodes in a liquid half-cell with a gas diffusion layer. Int Sci J Altern Energy Ecol 2:86–93

51. Astafiev EA, Dobrovolsky YA (2007) The behavior of membrane-electrode units of polymeric fuel cells: electrochemical methods to study catalytic activity and corrosion resistance of electrodes. Int Sci J Altern Energy Ecol 12:72–77

52. Chevalier S, Josset C, Bazylak A, Auvity B (2016) Measurements of air velocities in polymer electrolyte membrane fuel cell channels using electrochemical impedance spectroscopy. J Electrochemi Soc 163(8):F816–F823. https://doi.org/10.1149/2.0481608jes